RESEARCH ARTICLE

Duck Tembusu virus infection induces mitochondrial-mediated and death receptor-mediated apoptosis in duck embryo fibroblasts

Yuhong Pan[1,2,3†], Wenjun Cai[1,2,3†], Anchun Cheng[1,2,3*], Mingshu Wang[1,2,3], Shun Chen[1,2,3], Juan Huang[1,2,3], Qiao Yang[1,2,3], Ying Wu[1,2,3], Di Sun[1,2,3], Sai Mao[1,2,3], Dekang Zhu[1,2,3], Mafeng Liu[1,2,3], Xinxin Zhao[1,2,3], Shaqiu Zhang[1,2,3], Qun Gao[1,2,3], Xumin Ou[1,2,3], Bin Tian[1,3], Zhongqiong Yin[3] and Renyong Jia[1,2,3*]

Abstract

Duck Tembusu virus (DTMUV) is a pathogenic flavivirus that has caused enormous economic losses in Southeast Asia. Our previous study showed that DTMUV could induce duck embryo fibroblast (DEF) apoptosis, but the specific mechanism was not clear. In this study, we confirmed that DTMUV could induce the apoptosis of DEFs by DAPI staining and TUNEL staining. Furthermore, we found that the expression levels of cleaved-caspase-3/7/8/9 were significantly upregulated after DTMUV infection. After treatment of cells with an inhibitor of caspase-8 or caspase-9, DTMUV-induced apoptosis rates were significantly decreased, indicating that the caspase-8-mediated death receptor apoptotic pathway and caspase-9-mediated mitochondrial apoptotic pathway were involved in DTMUV-induced apoptosis. Moreover, we found that DTMUV infection not only caused the release of mitochondrial cytochrome C (Cyt C) and the downregulation of the apoptosis-inhibiting protein Bcl-2 but also reduced the mitochondrial membrane potential (MMP) and the accumulation of intracellular reactive oxygen species (ROS). Key genes in the mitochondrial apoptotic pathway and death receptor apoptotic pathway were upregulated to varying degrees, indicating the activation of the mitochondrial apoptosis pathway and death receptor apoptosis pathway. In conclusion, this study clarifies the molecular mechanism of DTMUV-induced apoptosis and provides a theoretical basis for revealing the pathogenic mechanism of DTMUV infection.

Keywords: DTMUV, apoptosis, DEF, mitochondrial apoptotic pathway

Introduction

DTMUV is an arbovirus of the genus *Flavivirus*, family *Flaviviridae* [1]. DTMUV is an enveloped virus with a positive-polarity RNA genome that is approximately

11 kb in length [2]. Beginning in April 2010, an outbreak of DTMUV occurred in major duck farming regions in China [3]. Since then, DTMUV has also caused serious harm to the duck industries in Thailand, Malaysia, and other Southeast Asian countries as well as China [4–6]. Slow growth of poultry, sharp declines in egg production, and even suspension of production have caused major economic losses [7]. Several studies have revealed that DTMUV has a wide host range, infecting ducks, chickens, geese, pigeons and house sparrows [8, 9]. Moreover, more than 70% of duck industry workers have been reported to

†Yuhong Pan and Wenjun Cai contributed equally to this work

*Correspondence: chenganchun@vip.163.com; jiary@sicau.edu.cn

[1] Research Center of Avian Disease, College of Veterinary Medicine, Sichuan Agricultural University, Chengdu 611130, Sichuan, China
Full list of author information is available at the end of the article

Pan *et al. Veterinary Research*   (2022) 53:53

Page 2 of 13

have antibodies against DTMUV in the serum samples tested, and ~50% of oral swab samples have been found to be positive for DTMUV RNA [10]. These findings indicate that DTMUV is likely to spread from ducks to other nonavian hosts and even humans. Therefore, it is necessary to explore the pathogenic mechanisms of DTMUV to enable the design of better disease control strategies.

Apoptosis, also known as programmed cell death (PCD), is a self-protective mechanism used by multicellular organisms to clear senescent, damaged or pathogen-infected cells [11]. Apoptotic cells are characterized by cell shrinkage, chromatin aggregation, DNA fragmentation, mitochondrial swelling, and ultimately the formation of apoptotic bodies containing nuclear or cytoplasmic debris surrounded by cell membranes and cleared by phagocytes [12].

Apoptosis has been shown to be induced by two classical pathways: the intrinsic and extrinsic pathways [13]. The chief players in the intrinsic pathway are mitochondria, the key energy producers of the cell [14]. The triggers for this apoptotic pathway are numerous and include DNA damage, oxidative damage, and endoplasmic reticulum stress (ERS) [15]. Infection with pathogens can also trigger intrinsic apoptosis through the aforementioned stresses [16]. These stimuli lead to the activation of Bax, which is mediated by BH3-only Bcl-2 family members such as Bim and PUMA [17, 18]. Bax activation manifests as oligomerization at the mitochondria, leading to the release of apoptotic proteins such as Cyt C [19] and endonuclease G (EndoG) [20]. Ultimately, this stimulates the formation of a multimeric complex composed of Apaf-1, Cyt C and procaspase-9, which is known as the apoptosome [21].

The extrinsic pathway is triggered through activation of extracellular death receptors of the tumour necrosis factor receptor (TNFR) superfamily, which bind specific ligands [22]. This family of receptors includes TNFR, Fas, death receptor 4 (DR4) and DR5 [23]. Upon activation of these receptors, initiator caspases such as pro-caspase-8 and pro-caspase-10 are recruited to the death receptor, where they become activated [24]. Critical to the formation of such complexes are the Fas-associated death domain (FADD) and TNF receptor-associated death domain (TRADD) proteins [25, 26]. These proteins act as adaptors that bridge death receptors and caspases. The complex of receptors, adaptors and caspases is typically referred to as the death-induced signalling complex (DISC) [27]. The formation of this complex leads to cleavage and activation of effector caspases such as caspase-3/7, whose protease activity directly acts on cellular substrates that are critical for the integrity of the cells [28]. Breakdown of these structural components leads to the hallmarks of apoptotic cell death, including nuclear DNA fragmentation, destruction of the cytoskeleton, blebbing and packing of cellular contents into small membrane-bound vesicles known as apoptotic bodies [29].

Apoptosis is a key innate defence mechanism that inhibits virus replication and clears virus-infected cells, which is important for maintaining healthy development of the body and normal function of the immune system [30]. However, many viruses have evolved strategies to prevent or delay apoptosis during viral replication until sufficient progeny viruses are produced [31]. In addition, some virus-induced apoptosis can also enhance viral spread, leading to tissue damage and disease. It has been found that a variety of flaviviruses, such as JEV, DENV, ZIKV, and WNV, can lead to apoptosis of host cells [32–35], and DTMUV, a new flavivirus, has similar biological properties. To address the uncertainties, this study preliminarily explored the molecular mechanism of induction of host cell apoptosis during DTMUV infection, providing a theoretical basis for revealing the pathogenic mechanism of DTMUV infection.

Materials and methods

Cells and viruses

DEFs were obtained from 10-day-old duck embryos according to the manufacturer's instructions [36]. The cells were grown in medium supplemented with 10% newborn bovine serum (NBS) (Gibco, Gaithersburg, MD, USA) and maintained in Dulbecco's modified Eagle's medium (DMEM) (Gibco Life Technologies, Shanghai, China) at 37 °C in a humidified atmosphere of 95% air and 5% CO_2. When the DEFs reached 90% confluence, they were mock-infected or infected with the DTMUV CQW1 strain (GenBank accession number KM233707.1) at a multiplicity of infection (MOI) of 1 [37, 38]. After the virus was adsorbed in a 37 °C, 5% CO_2 incubator for 1 h, the virus medium was replaced with maintenance medium (DMEM containing 2% NBS), and the cell samples were collected at the indicated time points. Each group was processed with three independent biological replicates.

DAPI staining of the cell nucleus

4′,6-Diamidino-2-phenylindole (DAPI) staining of the nucleus was conducted using a standard procedure. Briefly, DTMUV-infected and control cells were collected and fixed with 4% paraformaldehyde (PFA) for 1 h. Subsequently, the cells were permeabilized with 0.1% Triton X-100 for 30 min and stained with DAPI for 10 min. The nuclei were observed with a fluorescence microscope.

Pan *et al. Veterinary Research*   (2022) 53:53

Page 3 of 13

Terminal deoxynucleotidyl transferase-mediated dUTP nick end-labelling (TUNEL) assay

TUNEL staining was used to detect apoptosis-specific nuclear DNA fragmentation. Briefly, cells were fixed in 4% PFA for 30 min at room temperature, permeabilized for 5 min and washed with PBS three times. Then, the cells were stained using a TUNEL kit (Beyotime, China) according to the manufacturer's instructions. The slides were covered and incubated at 37 ℃ for 1 h in the dark. Finally, anti-fluorescein quenching solution was added. TUNEL-positive cells were visualized by green fluorescence, and images were observed under a fluorescence microscope.

Cell viability assays

Cell viability was measured using an MTT assay according to the manufacturer's instructions. Briefly, the cells were seeded in 96-well plates, and cell viability was detected at 36 h after IETD-FMK, Z-LEHD-FMK, and Z-VAD-FMK treatment.

Flow cytometric analysis of apoptosis

Apoptotic cells were detected by flow cytometry (FCM). The cells were washed twice with cold PBS and then resuspended in $1 \times$ binding buffer at a concentration of 1×10^6 cells/mL. Then, 100 μL of the solution (1×10^5 cells) was transferred to a 5 mL culture tube. Five microlitres of Annexin V-fluorescein isothiocyanate (V-FITC) (BD Pharmingen, USA) and 5 μL of propidium iodide (PI) (BD Pharmingen, USA) were added to 100 μL of cell suspension and incubated at RT (25 °C) in the dark for 15 min. Then, $1 \times$ binding buffer (400 μL) (BD Pharmingen, USA) was added to the mixture, and the percentage of apoptotic cells was assayed by FCM within 1 h.

Determination of MMP

Changes in cellular MMP were determined using a JC-10 staining kit (Sigma, USA). DEFs were seeded at a density of 2×10^6 cells in 6-well culture plates. After the adherent cells grew, they were infected with DTMUV or mock-infected for 12, 24, 36, 48 and 60 h at 37 °C in a CO_2 incubator. We prepared the JC-10 dye loading solution by adding 25 μL of $200 \times$ JC-10 to 5 mL of assay buffer. Then, adherent cells were detached with trypsin, collected by centrifugation, resuspended in 500 μL of the JC-10 dye loading solution and incubated at 37 °C in a 5% CO_2 incubator for 30 min protected from light. The stained cells were then collected by centrifugation and washed with assay buffer. After washing, the cell suspension was centrifuged once more and then resuspended in 1 mL assay buffer. Then, the cells were observed, and the data were collected with a fluorescence microscope and

a multifunctional microplate reader. When the MMP is high, JC-10 concentrates in the mitochondrial matrix, forming aggregates and generating red fluorescence. In apoptotic cells, MMP collapse results in the failure to retain JC-10 in the mitochondria; therefore, JC-10 becomes a monomer, producing green fluorescence. The relative ratio of red to green fluorescence was used to represent MMP.

Determination of intracellular ROS levels

Detection of intracellular ROS in DEFs was performed with a fluorometric intracellular ROS assay kit (Sigma–Aldrich, USA) based on a superoxide fluorescent probe (dihydroethidium). DEFs were plated in 96-well black microplates with clear flat bottoms to a cellular concentration of 1×10^4 cells/mL. The cells were then allowed to adhere for 24 h and infected with DTMUV, and the cells were harvested according to the instructions at 6, 12, 24, 36, 48 and 60 h of infection. The ROS reagent was reconstituted with dimethyl sulfoxide and then diluted in the assay buffer. Shortly afterwards, the ROS reagent solution was added to each well, and the plates were incubated for 1 h. Subsequently, the data were collected using a fluorescence microscope, and the fluorescence intensity was measured in a multifunctional microplate reader (Thermo Scientific, Massachusetts, USA) with an excitation wavelength of 520 nm and an emission wavelength of 605 nm. The data are shown as relative fluorescence compared to the fluorescence of the negative control.

Cytosolic fractionation

To detect the release of mitochondrial proteins, cell pellets were washed with cold PBS. Mitochondria were isolated using a Cell Mitochondria Isolation Kit (Beyotime, China). Briefly, cells were resuspended in lysis buffer and passed 10 times through a 26 G needle. The cell lysates were centrifuged, and both the supernatants and precipitates were collected. The protein concentrations of the cytosolic fraction (supernatant) and mitochondrial fraction (pellet) were determined with a BCA Protein Assay Kit (Beyotime, China). The protein samples were separated by SDS–PAGE for Western blotting.

Western blot analyses

Cells were cultured in 6-well plates and harvested with lysis buffer (Thermo Fisher Scientific, USA) containing a mixture of protease and phosphatase inhibitors. Equal amounts of the samples were then separated by SDS–PAGE (12% polyacrylamide), transferred to polyvinylidene difluoride membranes, and incubated with primary and secondary antibodies (rabbit antibodies against pro-caspase-3/7/8/9 were purchased from

Pan *et al. Veterinary Research*   (2022) 53:53

Page 4 of 13

ABclonal; antibodies against cleaved-caspase-3/7/8/9 were purchased from CST; a DTMUV-E mouse monoclonal antibody was prepared by our laboratory; antibodies against β-actin, PARP, Cyt C, VDAC1 were purchased from Proteintech; rabbit antibodies against Bcl-2 were purchased from Beyotime; and HRP-conjugated goat anti-mouse IgG and HRP-conjugated goat anti-rabbit IgG were purchased from Proteintech and visualized using an ECL system (Bio-Rad Laboratories)). The expression of β-actin, used as a loading control, was detected with an anti-β-actin mouse monoclonal antibody (Proteintech, China).

Total RNA was isolated from DTMUV-infected and mock-infected cells at different time points using TRIzol reagent (Invitrogen, CA, USA). The purity of all RNA samples was detected by analysing the A260/A280 ratio using a NanoDrop ND-1000 spectrophotometer (NanoDrop Technologies), which was expected to be 1.8–2.0. First-strand cDNA was obtained via reverse transcription of extracted RNA with a PrimeScript™ RT Reagent Kit (TAKARA). Q–RT–PCR was performed using a SYBR Green real-time PCR assay (CFX96 Bio-Rad, Hercules, CA, USA). The Q–RT–PCR was set up in a total volume of 20 μL containing 2 μL of cDNA, 10 μL of SYBR Premix (Tli RNaseH Plus), 1 μL of forward/reverse primer and 6 μL of ddH$_2$O. The duck β-actin gene was used as an internal control gene to normalize the targeted gene expression value. The quantity of mRNA was calculated by the $2^{-\Delta\Delta Ct}$ method and is presented as the mean ± SEM ($n=3$). The relative gene expression was calculated using the mean values obtained with the arithmetic formula ΔΔCt. The primers employed are listed in Table 1.

Statistical analysis

All experiments were performed in triplicate, and the data analysis was performed using GraphPad Prism 7.0. The results are expressed as the mean ± SEM, and statistical significance was assessed with Student's *t* test. *p* values less than 0.05 were considered to indicate statistical significance.
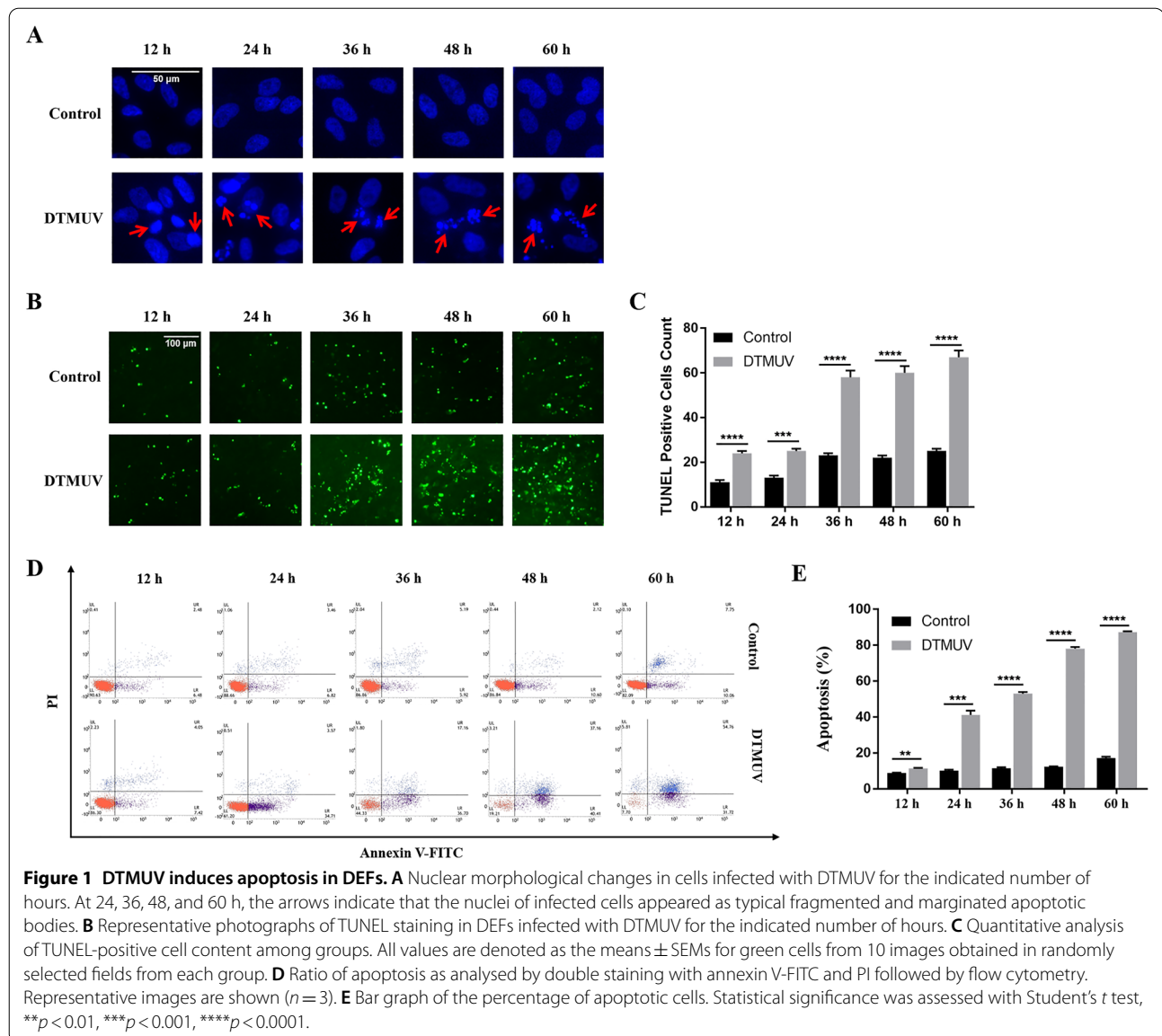
Results

DTMUV induces apoptosis in DEFs

DAPI staining was performed to observe the morphological changes in the cell nucleus (Figure 1A). The contraction of the nucleus and the aggregation of chromatin were observed at 12 and 24 h in the DTMUV-infected cells, which are denoted by arrowheads. In addition, DAPI staining at 24, 36, 48, and 60 h revealed the presence of apoptosis-associated morphological changes, such as nuclear fragmentation and apoptotic body formation.

When cells undergo apoptosis, some DNA endonucleases are activated, and these endonucleases cut off the genomic DNA between nucleosomes. When genomic DNA is broken, the exposed 3'-OH can be catalysed by terminal deoxynucleotidyl transferase (TdT) to add FITC-labelled dUTP (fluorescein-dUTP), which can be analysed by fluorescence microscopy. This is the principle of the TUNEL method to detect apoptosis. Compared with that in the control group, the green fluorescence in the group of DEFs infected with DTMUV increased significantly from 36 h, and the number of TUNEL-positive cells was increased after DTMUV infection, indicating that DTMUV infection can trigger the fragmentation of intracellular DNA and induce apoptosis (Figures 1B and

Table 1 Primers for Q–RT–PCR analysis of gene expression.

Target gene	Forward (5'-3')	Reverse (5'-3')
AIF	AGGCTGACACTCTTCCG	TCTGTGGTCCAGTTGCTC
XIAP	AGGCACTGACTATGACC	TCACTTTACAGCCTTCG
Apaf-1	AGAGGGCACAAGGAAGCTATCA	AACTTACTACCATCAGGCGAAACA
Smac	AGTCTGGCAGGTGGTG	CGTAACGCTGTCATCC
Bak	TCACCAAGGAGAATGCCTACGA	GCCTGTTATGCCGTGCTGGTA
Bcl-xL	AAAATGTCCAGCGGCAACC	AAGCCAACTCAGTCCTGTTCTCA
PARP	CTGGACTAAGTGCGTTGC	AGCCTCTGGAGGGAATA
Bid	CTGTCGCAGGCTGTGGAAGT	AGACACGCTGGAGAAGGAAGG
Cyt C	TGAGGATACCCTGATGGAGTACTTG	CTTCGCAGTGGCATCTTTCAG
FasL	AGCAGCCAGATGTTGAGCCA	GTCCCTCTCCCTGAGCTTGAATA
Fas	TATCTGCACTGACTTCAAGCGTATT	TGTTGGCTGTTGCATGACTGG
TNFSF10	CCCTGACACTTCCACG	CGATTCCCAGTTGCTTA
TNFRSF10B	TGCGAGATGTGCCAGAAGT	GGCGAAGACGTGGAAAGA
β-actin	GATCACAGCCCTGGCACC	CGGATTCATCATACTCCTGCTT

Pan *et al. Veterinary Research*   (2022) 53:53

Page 5 of 13

Figure 1 DTMUV induces apoptosis in DEFs. A Nuclear morphological changes in cells infected with DTMUV for the indicated number of hours. At 24, 36, 48, and 60 h, the arrows indicate that the nuclei of infected cells appeared as typical fragmented and marginated apoptotic bodies. **B** Representative photographs of TUNEL staining in DEFs infected with DTMUV for the indicated number of hours. **C** Quantitative analysis of TUNEL-positive cell content among groups. All values are denoted as the means ± SEMs for green cells from 10 images obtained in randomly selected fields from each group. **D** Ratio of apoptosis as analysed by double staining with annexin V-FITC and PI followed by flow cytometry. Representative images are shown (*n* = 3). **E** Bar graph of the percentage of apoptotic cells. Statistical significance was assessed with Student's *t* test, ***p* < 0.01, ****p* < 0.001, *****p* < 0.0001.
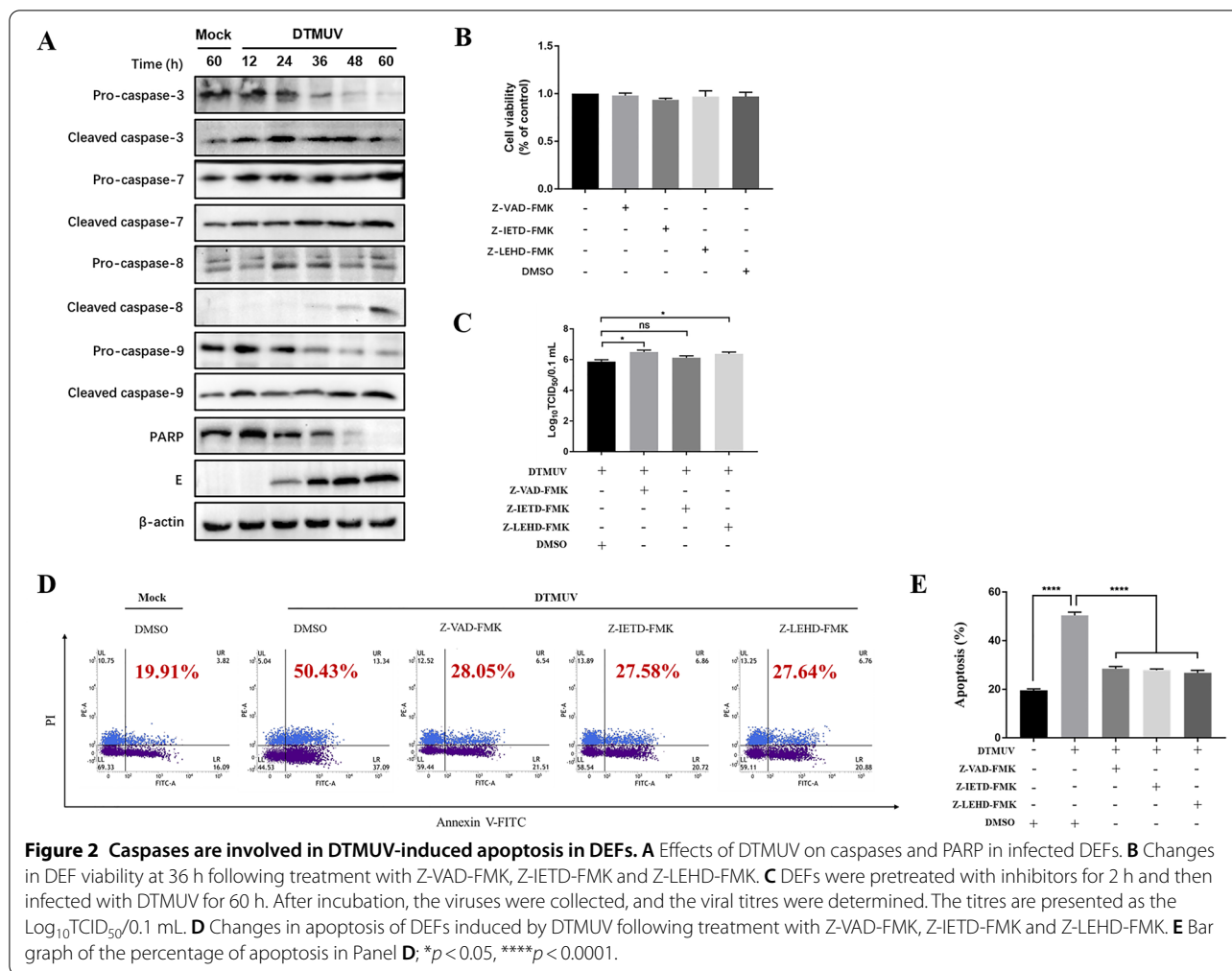
C). Flow cytometric analysis was performed after staining with Annexin V-FITC and PI, and the results showed that DTMUV had a significant proapoptotic effect that was obviously time-dependent (Figures 1D and E).

Caspases are involved in DTMUV-induced apoptosis in DEFs

Activation of caspases is essential during apoptosis. It is well known that mitochondria-mediated and death receptor-mediated pathways induce apoptosis via caspase-9 and caspase-8, respectively, and the apoptosis effector molecule is caspase-3/7. To determine the molecular mechanism of DTMUV-induced apoptosis, we first explored the roles of the caspases in the process

of apoptosis and analysed the pathway through which DTMUV induced apoptosis. The DTMUV-E protein was used to indicate the virus infection process. The results are shown in Figure 2A. DTMUV infection promoted increased expression of cleaved caspase-3, caspase-7, caspase-8 and caspase-9. In addition, the DNA repair enzyme PARP (poly(ADP-ribose) polymerase), which serves as a substrate for cleaved caspase-3/7, was inactivated by cleavage.

To further determine the roles of caspases in apoptosis, an MTT assay was used to detect the effects of Z-IETD-FMK, Z-LEHD-FMK and Z-VAD-FMK on cell viability. The results showed that the above inhibitors had no effect on DEF viability (Figure 2B). Then, we

Pan *et al. Veterinary Research*   (2022) 53:53

Page 6 of 13

Figure 2 Caspases are involved in DTMUV-induced apoptosis in DEFs. A Effects of DTMUV on caspases and PARP in infected DEFs. **B** Changes in DEF viability at 36 h following treatment with Z-VAD-FMK, Z-IETD-FMK and Z-LEHD-FMK. **C** DEFs were pretreated with inhibitors for 2 h and then infected with DTMUV for 60 h. After incubation, the viruses were collected, and the viral titres were determined. The titres are presented as the $Log_{10}TCID_{50}$/0.1 mL. **D** Changes in apoptosis of DEFs induced by DTMUV following treatment with Z-VAD-FMK, Z-IETD-FMK and Z-LEHD-FMK. **E** Bar graph of the percentage of apoptosis in Panel **D**; $*p < 0.05$, $****p < 0.0001$.

assessed the effects of Z-VAD-FMK, Z-LEHD-FMK and Z-LEHD-FMK on viral replication. The results in Figure 2C show that Z-VAD-FMK and Z-LEHD-FMK effectively promoted viral replication, whereas Z-IETD-FMK had a weak effect on viral replication. Subsequently, the cells were pretreated with specific inhibitors of caspase-8 and caspase-9, Z-IETD-FMK and Z-LEHD-FMK, and the broad-spectrum caspase inhibitor Z-VAD-FMK and then infected with DTMUV for 36 h. Afterwards, it was determined whether Z-IETD-FMK, Z-LEHD-FMK and Z-VAD-FMK could inhibit DTMUV-induced apoptosis. We found that the specific inhibitors of caspase-8 and caspase-9, Z-IETD-FMK and Z-LEHD-FMK, and the broad-spectrum caspase inhibitor Z-VAD-FMK all inhibited DTMUV-induced apoptosis (Figures 2D and E). The above results show that DTMUV infection of DEFs promotes the activation of caspase-8 and caspase-9 cleavage and that specific inhibitors of caspase-8 or caspase-9 can inhibit apoptosis, indicating that infection activates the caspase-9-mediated mitochondrial apoptotic pathway

and the caspase-8-mediated death receptor apoptotic pathway.

DTMUV induces a decrease in MMP

Depolarization of MMP is one of the earliest symptoms of mitochondria-mediated apoptosis [39]. Previous results have suggested that the mitochondrial pathway is involved in DTMUV-induced apoptosis. To further qualitatively confirm that DTMUV-induced DEF apoptosis occurs through the endogenous mitochondrial pathway, we used JC-10 probe technology to detect the MMP. In normal cells, in which the MMP is high, JC-1 aggregates in the mitochondria, forming polymers and emitting red fluorescence. In contrast, in apoptotic cells, in which the MMP is reduced, JC-10 cannot aggregate in the mitochondria and remains in the monomeric form, emitting green fluorescence. A decrease in MMP is a hallmark of apoptosis occurring through the mitochondrial pathway, as shown in Figure 3. It was observed by fluorescence microscopy that the red fluorescence was decreased and
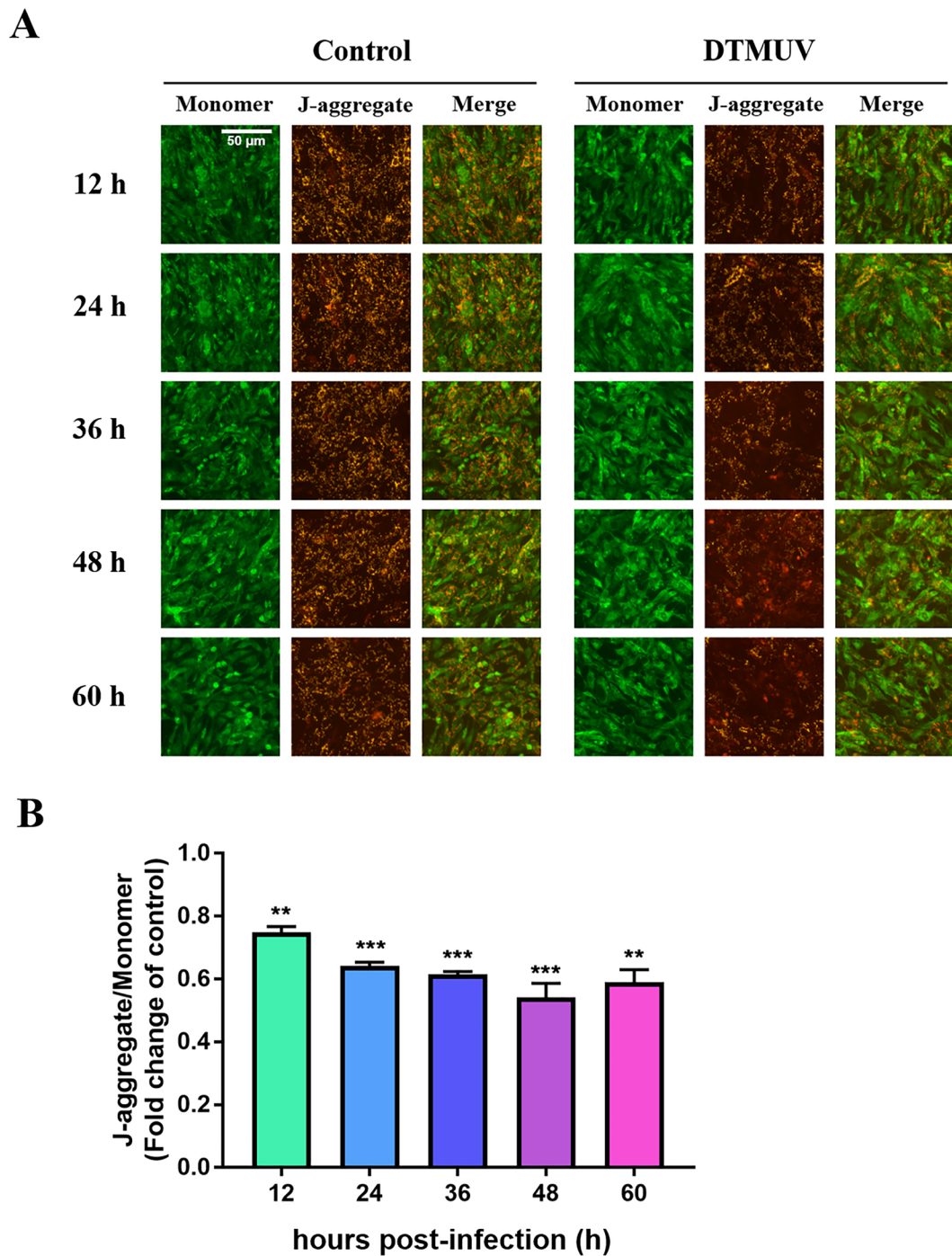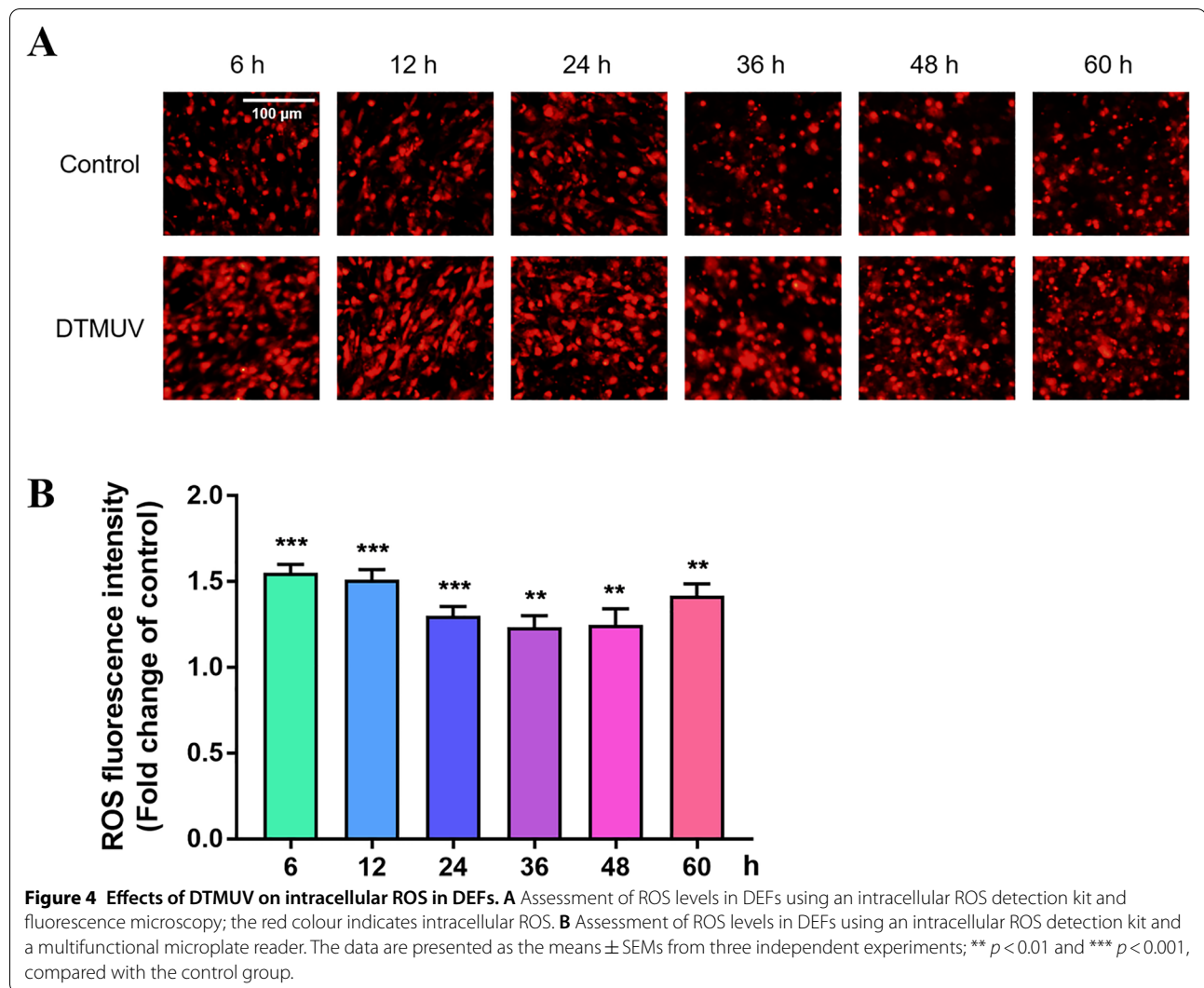
Pan *et al. Veterinary Research*   (2022) 53:53

Page 7 of 13

Figure 3 Mitochondrial membrane potential (MMP) determination in DEFs. **A** Assessment of DEF cell MMP through JC-10 staining and fluorescence microscopy. Mitochondria with normal membrane potential are indicated in red, and mitochondria with reduced membrane potential are indicated in green. **B** Assessment of DEF MMP with JC-10 staining and a multifunctional microplate reader. The data are presented as the means ± SEMs from three independent experiments. **$p < 0.01$ and ***$p < 0.001$, compared with the control group.

the green fluorescence was increased significantly at 12, 24, 36, 48 and 60 h after DTMUV infection compared to the fluorescence in the control group, which indicates that DTMUV leads to the depolarization of MMP.

DTMUV causes accumulation of intracellular ROS

ROS are produced by the mitochondria, and increased ROS levels reduce the MMP, which activates the mitochondrial apoptotic pathway. The results in Figure 3
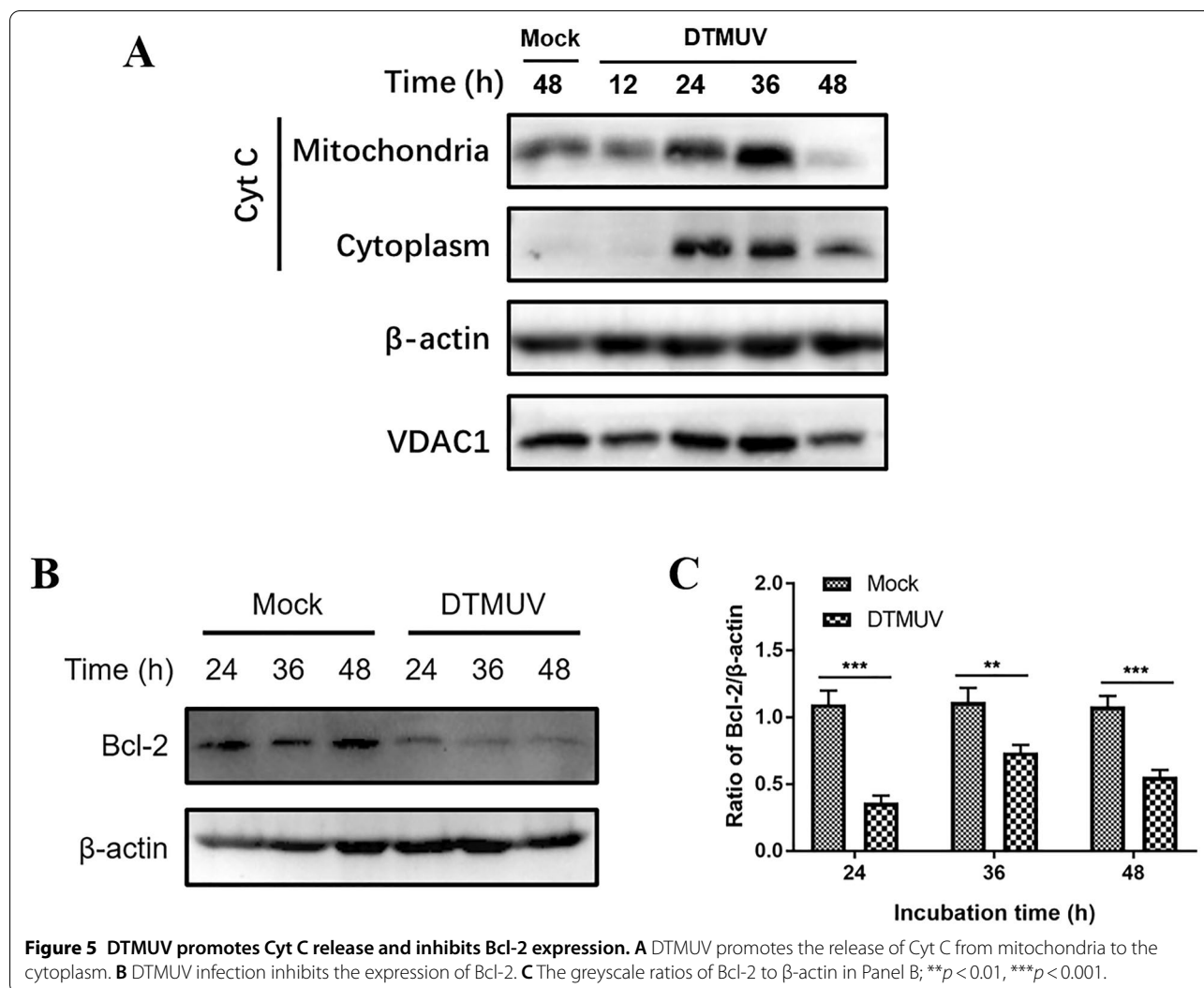
Pan *et al. Veterinary Research*   (2022) 53:53

Page 8 of 13

Figure 4 **Effects of DTMUV on intracellular ROS in DEFs. A** Assessment of ROS levels in DEFs using an intracellular ROS detection kit and fluorescence microscopy; the red colour indicates intracellular ROS. **B** Assessment of ROS levels in DEFs using an intracellular ROS detection kit and a multifunctional microplate reader. The data are presented as the means ± SEMs from three independent experiments; ** $p < 0.01$ and *** $p < 0.001$, compared with the control group.

show that DTMUV can lead to MMP depolarization. On this basis, we further tested whether DTMUV can cause intracellular ROS accumulation. A ROS detection kit was used to detect intracellular ROS, and the images collected by fluorescence microscopy showed that after DTMUV infection of DEFs for 6, 12, 24, 36, 48 and 60 h, the red fluorescence was enhanced compared with that of the control group (Figure 4A). The red fluorescence values detected by the microplate reader at 6, 12, 24, 36, 48 and 60 h after DTMUV infection were higher than those in the control group, and there were significant differences (Figure 4B). The results indicate that DTMUV can induce an increase in intracellular ROS and promote the occurrence of apoptosis.

DTMUV promotes Cyt C release and inhibits Bcl-2 expression

Cyt C release plays a central role in mitochondria-mediated apoptosis. The expression of Cyt C protein in the mitochondria and cytoplasm was detected by Western blotting, and DTMUV promoted the release of Cyt C from mitochondria into the cytoplasm, which confirmed that the basic structure of cell mitochondria had been destroyed (Figure 5A). The results indicate that DTMUV can induce apoptosis through the mitochondria-mediated apoptotic pathway.

The Bcl-2 protein family is an important family of regulatory proteins that regulate mitochondrial apoptosis, and the Bcl-2 protein has an antiapoptotic function.

Figure 5 DTMUV promotes Cyt C release and inhibits Bcl-2 expression. **A** DTMUV promotes the release of Cyt C from mitochondria to the cytoplasm. **B** DTMUV infection inhibits the expression of Bcl-2. **C** The greyscale ratios of Bcl-2 to β-actin in Panel B; **$p < 0.01$, ***$p < 0.001$.

Therefore, this study continued to detect the expression of Bcl-2, and the results showed that the expression of Bcl-2 protein was significantly decreased, indicating that DTMUV infection can inhibit the expression of the antia-poptotic protein Bcl-2 to promote apoptosis (Figures 5B and C).

Changes in the mRNA levels of key genes in the mitochondrial apoptotic pathway

To determine the mRNA changes in mitochondrial apoptotic pathway-related cytokines, Q–RT–PCR was used to detect the mRNA levels of key mitochondrial pathway genes. The results showed that the mRNA levels of the proapoptotic factor Apaf-1 and the antiapoptotic protein XIAP were significantly increased at 12, 24, 36, 48 and 60 h. The mRNA levels of other proapoptotic factors were also increased: the AIF mRNA level was increased at 48 and 60 h, the Smac mRNA level was significantly increased at 36 and 48 h, and the Cyt C mRNA level was obviously increased at 24, 36, 48 and 60 h. Although the PARP protein level was downregulated, its mRNA level was obviously higher than that of the control group at 12, 24, 36 and 48 h. The mRNA levels of Bcl-2 family members (Bid, Bak, Bcl-xL) involved in the regulation of the mitochondrial apoptotic pathway were upregulated at different time points after DTMUV infection (Figure 6). The above results further confirm the activation of the mitochondrial pathway.

Changes in the mRNA levels of key genes in the death receptor apoptotic pathway

Furthermore, we also used Q–RT–PCR to detect the mRNA levels of key genes in the death receptor apoptotic pathway. Compared with those in the control group, FasL and TNFRSF10B mRNA levels were upregulated at

Pan *et al. Veterinary Research*   (2022) 53:53

Page 10 of 13

Figure 6 mRNA expression levels of the mitochondrial pathway genes AIF, XIAP, Apaf-1, Smac, Bak, Bcl-xL, PARP1, Bid and Cyt C. *$p < 0.05$, **$p < 0.01$, ***$p < 0.001$, ****$p < 0.0001$.
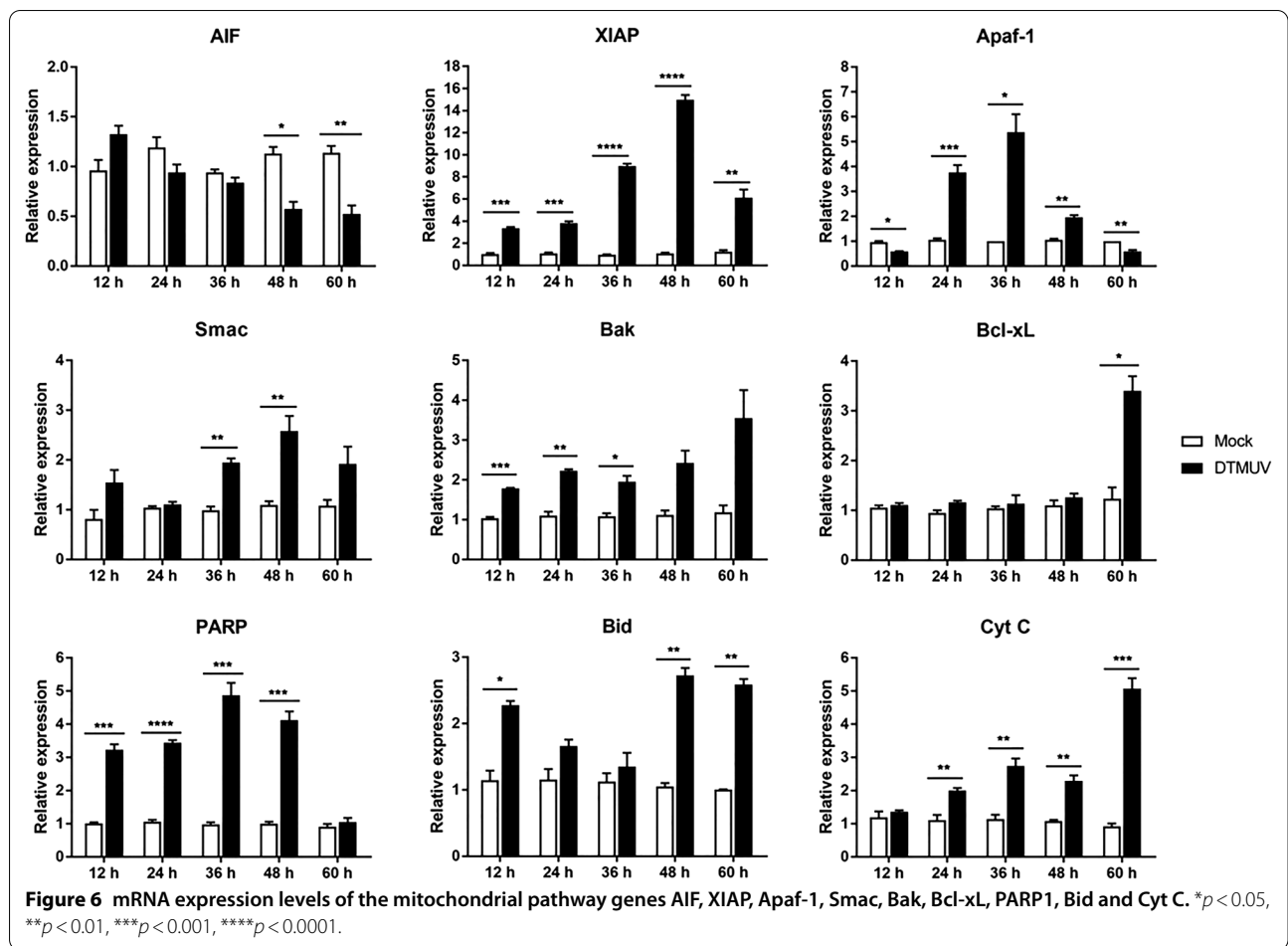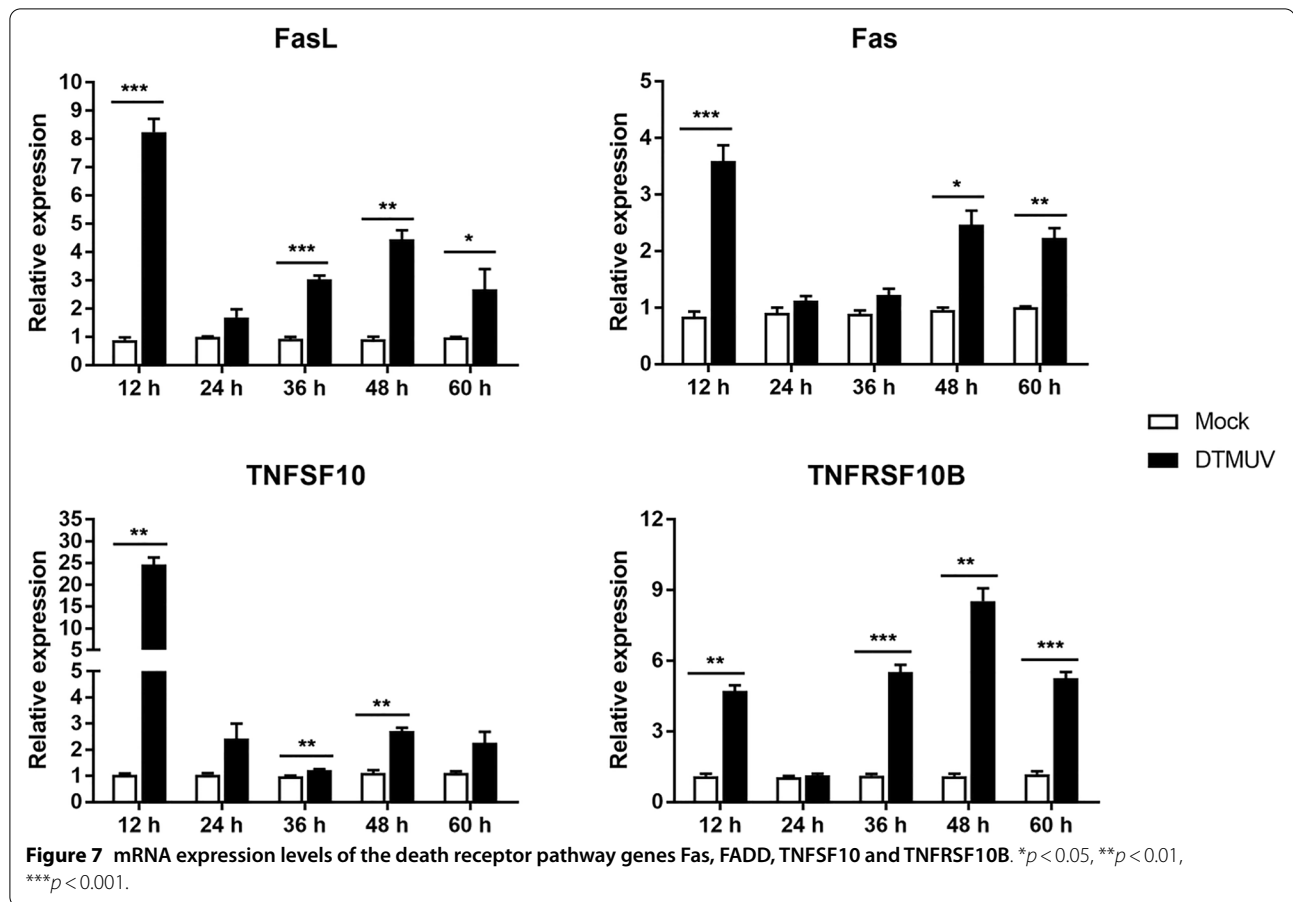
12, 36, 48 and 60 h. The Fas mRNA level was significantly increased at 12, 48 and 60 h, and the TNFSF10 mRNA level was obviously increased at 12, 36 and 48 h compared with that in the control group (Figure 7), which further confirms the activation of the death receptor apoptotic pathway.

Discussion

Previous research by our group has shown that DTMUV infection can induce the apoptosis of DEFs [9], and DEF apoptosis induced by virus infection is typically time-dependent, but the signalling pathway of DTMUV-induced DEF apoptosis has not been thoroughly investigated. In this study, the cytopathic changes of DEFs were first observed by fluorescence microscopy, and it was found that virus infection caused the typical morphological changes of apoptosis, such as shrinkage of DEFs, pyknosis of the nucleus, and rupture of the nucleus. In addition, a TUNEL assay showed that DTMUV infection induced DNA fragmentation. The above results verify that DTMUV infection can induce significant apoptosis in DEFs. The classical apoptosis pathways can be divided

into the mitochondria-mediated apoptotic pathway and the death receptor-mediated apoptotic pathway [40]. Caspases play important roles in the process of apoptosis. Caspase-9 and caspase-8 are involved in the mitochondrial apoptotic pathway and death receptor apoptotic pathway, respectively [41]. They can activate the downstream protein caspase-3/7 to execute apoptosis [42]. In this study, we found that DTMUV can activate caspase-3, caspase-7, caspase-8 and caspase-9. We treated cells with specific inhibitors of caspase-8 and caspase-9 (Z-IETD-FMK and Z-LEHD-FMK, respectively) and a broad-spectrum caspase inhibitor (Z-VAD-FMK). We found that the specific inhibitors of caspase-8 and caspase-9 and the broad-spectrum caspase inhibitor all inhibited DTMUV-induced apoptosis. This indicated that the caspase-8-mediated death receptor apoptotic pathway and the caspase-9-mediated mitochondrial apoptotic pathway were involved in DTMUV-induced apoptosis. Moreover, we found that virus titres were upregulated after Z-VAD-FMK and Z-LEHD-FMK pretreatment of cells, suggesting that inhibition of apoptosis contributes to DTMUV replication.

Pan *et al. Veterinary Research*   (2022) 53:53

Page 11 of 13

Figure 7 mRNA expression levels of the death receptor pathway genes Fas, FADD, TNFSF10 and TNFRSF10B. *$p < 0.05$, **$p < 0.01$, ***$p < 0.001$.

Mitochondria are organelles with a double-membrane structure. The outer membrane is more permeable than the inner membrane, allowing molecules or ions less than 5 kDa to pass through [43]. The difference in permeability between the outer and inner mitochondrial membranes is a key factor in maintaining MMP [44]. The mitochondrial apoptotic pathway is mainly caused by regulation of the mitochondrial release of Cyt C [45]. Cyt C released from mitochondria binds to Apaf-1 to activate caspase-9 and then activate downstream caspase3/7 [46]; this pathway is usually accompanied by changes in MMP [47]. The accumulation of intracellular ROS can activate mitochondrial permeability transition pore (MPTP) opening and MMP depolarization [48], while MPTP opening and MMP decrease can lead to oxidative phosphorylation and deoxygenation on mitochondria, resulting in blockade of ATP synthesis and a sharp increase in intracellular ROS [49]. Infection of porcine testicular cells (ST cells) with PDCoV results in the opening of the MPTP, the depolarization of MMP and the release of Cyt C from mitochondria into the cytoplasm, inducing apoptosis [50]. After confirming that DTMUV can activate caspase-9, we found that DTMUV infection of DEFs

can promote the release of Cyt C from mitochondria to the cytoplasm and can also inhibit the expression of the antiapoptotic protein Bcl-2. In addition, according to the JC-10 probe detection results, DTMUV infection can cause the host MMP to decrease. The reduction in MMP helps to release apoptosis-related substances such as Cyt C, Smac, and AIF in mitochondria into the cytoplasm to ultimately induce apoptosis [51]. This finding indicates that DTMUV can induce apoptosis through the mitochondrial apoptotic pathway.

ROS are free radicals mainly produced by mitochondria, including superoxide anions, hydrogen peroxide, hydroxyl radicals, etc. Studies have found that ROS are involved in important biological processes, such as cell proliferation, apoptosis and autophagy [52]. Under normal circumstances, ROS are in a dynamic equilibrium. If cells are stimulated, the increase in ROS content will lead to intracellular oxidative stress, which can directly attack the MMP and trigger the release of Cyt C from mitochondria [53]. ROS can also directly affect macromolecules such as cellular DNA, resulting in DNA breakage and apoptosis [54]. This study shows that DTMUV infection can promote the accumulation

Pan *et al. Veterinary Research*   (2022) 53:53

Page 12 of 13

of intracellular ROS, but the exact mechanism by which DTMUV regulates the accumulation of ROS is still unclear; it may involve the regulation of mitochondrial ROS metabolism enzymes. In addition, Q–RT–PCR detection showed that the mRNA levels of key factors of the mitochondrial apoptotic pathway and death receptor apoptotic pathway were upregulated to varying degrees after DTMUV infection. The above results indicate that DTMUV infection of host cells induces apoptosis through the mitochondria-mediated apoptotic pathway and death receptor-mediated apoptotic pathway, revealing the molecular mechanism of DTMUV infection-induced host cell apoptosis.

DTMUV infection triggers typical lesions of apoptosis, and caspase-8 and caspase-9 are involved in DTMUV-induced apoptosis. DTMUV activates the mitochondria-mediated apoptotic pathway by triggering the release of mitochondrial Cyt C, inhibiting the expression of the antiapoptotic protein Bcl-2, decreasing MMP and inducing intracellular ROS accumulation. In addition, the expression levels of key factors in the mitochondrial apoptotic pathway and death receptor apoptotic pathway are upregulated to varying degrees, indicating the activation of the mitochondrial apoptotic pathway and the death receptor apoptotic pathway. This study clarifies the molecular mechanism of apoptosis induced by DTMUV and provides a theoretical basis for revealing the pathogenic mechanism of DTMUV infection.

Abbreviations
DTMUV: Duck Tembusu virus; DEF: Duck embryo fibroblast; Cyt C: cytochrome C; MMP: mitochondrial membrane potential; ROS: reactive oxygen species; PCD: programmed cell death; ERS: endoplasmic reticulum stress; EndoG: endonuclease G; TNFR: tumour necrosis factor receptor; DR: death receptor; FADD: Fas-associated death domain; TRADD: TNF receptor-associated death domain; DISC: death-induced signalling complex; NBS: newborn bovine serum; DMEM: Dulbecco's modified Eagle's medium; MOI: multiplicity of infection; TUNEL: terminal deoxynucleotidyl transferase-mediated dUTP nick end-labelling; PFA: paraformaldehyde; FCM: flow cytometry; V-FITC: annexin V-fluorescein isothiocyanate; PI: propidium iodide; TdT: terminal deoxynucleotidyl transferase; PARP: poly (ADP-ribose) polymerase; MPTP: mitochondrial permeability transition pore.

Authors' contributions
Conceptualization, YP; methodology, YP and WC; software, YP and WC; validation, RJ; formal analysis, YP; investigation, YP; resources, SC, DZ, ML, XZ, SZ, DS and ZY; data curation, YP; writing-original draft preparation, YP; writing-review and editing, RJ; visualization, QY, YW, JH, SM, XO, QG and BT; supervision, RJ; project administration, RJ and AC; funding acquisition, RJ, AC and MW. All authors read and approved the final manuscript.

Declarations

Ethics approval and consent to participate
The animal studies were approved by the Institutional Animal Care and Use Committee of Sichuan Agricultural University, Sichuan, China, and followed the National Institutes of Health guidelines for the performance of animal experiments.

Competing interests
The authors declare that they have no competing interests.

Author details
[1]Research Center of Avian Disease, College of Veterinary Medicine, Sichuan Agricultural University, Chengdu 611130, Sichuan, China. [2]Institute of Preventive Veterinary Medicine, Sichuan Agricultural University, Chengdu 611130, Sichuan, China. [3]Key Laboratory of Animal Disease and Human Health of Sichuan Province, Chengdu 611130, Sichuan, China.

References
1. Li N, Zhao J, Yang Y, Zeng Y, Liu S (2020) Innate immune responses to duck Tembusu virus infection. Vet Res 51:87
2. Lei W, Guo X, Fu S, Feng Y, Tao X, Gao X, Song J, Yang Z, Zhou H, Liang G (2017) The genetic characteristics and evolution of Tembusu virus. Vet Microbiol 201:32–41
3. Su J, Li S, Hu X, Yu X, Wang Y, Liu P, Lu X, Zhang G, Hu X, Liu D, Li X, Su W, Lu H, Mok NS, Wang P, Wang M, Tian K, Gao GF (2011) Duck egg-drop syndrome caused by BYD virus, a new Tembusu-related flavivirus. PLoS One 6:e18106
4. Thontiravong A, Ninvilai P, Tunterak W, Nonthabenjawan N, Chaiyavong S, Angkabkingkaew K, Mungkundar C, Phuengpho W, Oraveerakul K, Amonsin A (2015) Tembusu-related Flavivirus in Ducks, Thailand. Emerg Infect Dis 21:2164–2167
5. Yan P, Zhao Y, Zhang X, Xu D, Dai X, Teng Q, Yan L, Zhou J, Ji X, Zhang S, Liu G, Zhou Y, Kawaoka Y, Tong G, Li Z (2011) An infectious disease of ducks caused by a newly emerged Tembusu virus strain in mainland China. Virology 417:1–8
6. Zhang W, Chen S, Mahalingam S, Wang M, Cheng A (2017) An updated review of avian-origin Tembusu virus: a newly emerging avian Flavivirus. J Gen Virol 98:2413–2420
7. Menicucci AR, Versteeg K, Woolsey C, Mire CE, Geisbert JB, Cross RW, Agans KN, Jankeel A, Geisbert TW, Messaoudi I (2017) Transcriptome analysis of circulating immune cell subsets highlight the role of monocytes in Zaire Ebola Virus Makona pathogenesis. Front Immunol 8:1372
8. Tang Y, Diao Y, Yu C, Gao X, Ju X, Xue C, Liu X, Ge P, Qu J, Zhang D (2013) Characterization of a Tembusu virus isolated from naturally infected house sparrows (*Passer domesticus*) in Northern China. Transbound Emerg Dis 60:152–158
9. Pan Y, Cheng A, Zhang X, Wang M, Chen S, Zhu D, Liu M, Zhao X, Yang Q, Wu Y, Huang J, Zhang S, Mao S, Ou X, Gao Q, Yu Y, Liu Y, Zhang L, Yin Z, Jing B, Tian B, Pan L, Rehman MU, Chen X, Jia R (2020) Transcriptome analysis of duck embryo fibroblasts for the dynamic response to duck tembusu virus infection and dual regulation of apoptosis genes. Aging 12:17503–17527
10. Tang Y, Gao X, Diao Y, Feng Q, Chen H, Liu X, Ge P, Yu C (2013) Tembusu virus in human, China. Transbound Emerg Dis 60:193–196
11. Bertheloot D, Latz E, Franklin BS (2021) Necroptosis, pyroptosis and apoptosis: an intricate game of cell death. Cell Mol Immunol 18:1106–1121
12. Kennedy PGE (2015) Viruses, apoptosis, and neuroinflammation—a double-edged sword. J Neurovirol 21:1–7
13. Ashkenazi A, Salvesen G (2014) Regulated cell death: signaling and mechanisms. Annu Rev Cell Dev Biol 30:337–356
14. Wong WW-L, Puthalakath H (2008) Bcl-2 family proteins: the sentinels of the mitochondrial apoptosis pathway. IUBMB Life 60:390–397
15. Verma G, Datta M (2012) The critical role of JNK in the ER-mitochondrial crosstalk during apoptotic cell death. J Cell Physiol 227:1791–1795

Pan *et al. Veterinary Research*   (2022) 53:53

Page 13 of 13

16. Borner C, Andrews DW (2014) The apoptotic pore on mitochondria: are we breaking through or still stuck? Cell Death Differ 21:187–191

17. Papaianni E, El Maadidi S, Schejtman A, Neumann S, Maurer U, Marino-Merlo F, Mastino A, Borner C (2015) Phylogenetically distant viruses use the same BH3-only protein puma to trigger Bax/Bak-dependent apoptosis of infected mouse and human cells. PLoS One 10:e0126645

18. Kilbride SM, Prehn JHM (2013) Central roles of apoptotic proteins in mitochondrial function. Oncogene 32:2703–2711

19. Garrido C, Galluzzi L, Brunet M, Puig PE, Didelot C, Kroemer G (2006) Mechanisms of cytochrome c release from mitochondria. Cell Death Differ 13:1423–1433

20. Jang DS, Penthala NR, Apostolov EO, Wang X, Crooks PA, Basnakian AG (2015) Novel cytoprotective inhibitors for apoptotic endonuclease G. DNA Cell Biol 34:92–100

21. Yuan S, Akey CW (2013) Apoptosome structure, assembly, and procaspase activation. Structure 21:501–515

22. Locksley RM, Killeen N, Lenardo MJ (2001) The TNF and TNF receptor superfamilies: integrating mammalian biology. Cell 104:487–501

23. Rubio-Moscardo F, Blesa D, Mestre C, Siebert R, Balasas T, Benito A, Rosenwald A, Climent J, Martinez JI, Schilhabel M, Karran EL, Gesk S, Esteller M, deLeeuw R, Staudt LM, Fernandez-Luna JL, Pinkel D, Dyer MJS, Martinez-Climent JA (2005) Characterization of 8p21.3 chromosomal deletions in B-cell lymphoma: TRAIL-R1 and TRAIL-R2 as candidate dosage-dependent tumor suppressor genes. Blood 106:3214–3222

24. Müller DN, Binger KJ, Riediger F (2012) Prorenin receptor regulates more than the renin-angiotensin system. Ann Med 44:S43–S48

25. Suliman A, Lam A, Datta R, Srivastava RK (2001) Intracellular mechanisms of TRAIL: apoptosis through mitochondrial-dependent and -independent pathways. Oncogene 20:2122–2133

26. Huang K, Zhang J, O'Neill KL, Gurumurthy CB, Quadros RM, Tu Y, Luo X (2016) Cleavage by caspase 8 and mitochondrial membrane association activate the BH3-only protein Bid during TRAIL-induced apoptosis. J Biol Chem 291:11843–11851

27. Kischkel FC, Hellbardt S, Behrmann I, Germer M, Pawlita M, Krammer PH, Peter ME (1995) Cytotoxicity-dependent APO-1 (Fas/CD95)-associated proteins form a death-inducing signaling complex (DISC) with the receptor. EMBO J 14:5579–5588

28. Ashkenazi A (2008) Targeting the extrinsic apoptosis pathway in cancer. Cytokine Growth Factor Rev 19:325–331

29. Pobezinskaya YL, Liu Z (2012) The role of TRADD in death receptor signaling. Cell Cycle 11:871–876

30. Benedict CA, Norris PS, Ware CF (2002) To kill or be killed: viral evasion of apoptosis. Nat Immunol 3:1013–1018

31. Orzalli MH, Prochera A, Payne L, Smith A, Garlick JA, Kagan JC (2021) Virus-mediated inactivation of anti-apoptotic Bcl-2 family members promotes gasdermin-E-dependent pyroptosis in barrier epithelial cells. Immunity 54:1447-1462.e5

32. Slomnicki LP, Chung D-H, Parker A, Hermann T, Boyd NL, Hetman M (2017) Ribosomal stress and Tp53-mediated neuronal apoptosis in response to capsid protein of the Zika virus. Sci Rep 7:16652

33. Bhattacharyya S, Sen U, Vrati S (2014) Regulated IRE1-dependent decay pathway is activated during Japanese encephalitis virus-induced unfolded protein response and benefits viral replication. J Gen Virol 95:71–79

34. Huang J, Li Y, Qi Y, Zhang Y, Zhang L, Wang Z, Zhang X, Gui L (2014) Coordinated regulation of autophagy and apoptosis determines endothelial cell fate during Dengue virus type 2 infection. Mol Cell Biochem 397:157–165

35. Shrestha B, Gottlieb D, Diamond MS (2003) Infection and injury of neurons by West Nile encephalitis virus. J Virol 77:13203–13213

36. Adams S, Xing Z, Li J, Mendoza K, Perez D, Reed K, Cardona C (2013) The effect of avian influenza virus NS1 allele on virus replication and innate gene expression in avian cells. Mol Immunol 56:358–368

37. Chen S, He Y, Zhang R, Liu P, Yang C, Wu Z, Zhang J, Wang M, Jia R, Zhu D, Liu M, Yang Q, Wu Y, Cheng A (2018) Establishment of a reverse genetics system for duck Tembusu virus to study virulence and screen antiviral genes. Antiviral Res 157:120–127

38. Zhu K, Huang J, Jia R, Zhang B, Wang M, Zhu D, Chen S, Liu M, Yin Z, Cheng A (2015) Identification and molecular characterization of a novel duck Tembusu virus isolate from Southwest China. Arch Virol 160:2781–2790

39. Tait SWG, Green DR (2010) Mitochondria and cell death: outer membrane permeabilization and beyond. Nat Rev Mol Cell Biol 11:621–632

40. Pan Y, Cheng A, Wang M, Yin Z, Jia R (2021) The dual regulation of apoptosis by flavivirus. Front Microbiol 12:654494

41. Nagata S (2018) Apoptosis and clearance of apoptotic cells. Annu Rev Immunol 36:489–517

42. Beroske L, Van den Wyngaert T, Stroobants S, Van der Veken P, Elvas F (2021) Molecular imaging of apoptosis: the case of caspase-3 radiotracers. Int J Mol Sci 22:3948

43. Burke PJ (2017) Mitochondria, bioenergetics and apoptosis in cancer. Trends Cancer 3:857–870

44. Kalpage HA, Bazylianska V, Recanati MA, Fite A, Liu J, Wan J, Mantena N, Malek MH, Podgorski I, Heath EI, Vaishnav A, Edwards BF, Grossman LI, Sanderson TH, Lee I, Hüttemann M (2019) Tissue-specific regulation of cytochrome c by post-translational modifications: respiration, the mitochondrial membrane potential, ROS, and apoptosis. FASEB J 33:1540–1553

45. Bock FJ, Tait SWG (2020) Mitochondria as multifaceted regulators of cell death. Nat Rev Mol Cell Biol 21:85–100

46. Brazeau E, Mahalingam R, Gilden D, Wellish M, Kaufer BB, Osterrieder N, Pugazhenthi S (2010) Varicella-zoster virus-induced apoptosis in MeWo cells is accompanied by down-regulation of Bcl-2 expression. J Neurovirol 16:133–140

47. Yang F, Pei R, Zhang Z, Liao J, Yu W, Qiao N, Han Q, Li Y, Hu L, Guo J, Pan J, Tang Z (2019) Copper induces oxidative stress and apoptosis through mitochondria-mediated pathway in chicken hepatocytes. Toxicol In Vitro 54:310–316

48. Bernardi P (1992) Modulation of the mitochondrial cyclosporin A-sensitive permeability transition pore by the proton electrochemical gradient. Evidence that the pore can be opened by membrane depolarization. J Biol Chem 267:8834–8839

49. Yu T, Zhen M, Li J, Zhou Y, Ma H, Jia W, Wang C (2019) Anti-apoptosis effect of amino acid modified gadofullerene via a mitochondria mediated pathway. Dalton Trans 48:7884–7890

50. Lee YJ, Lee C (2018) Porcine deltacoronavirus induces caspase-dependent apoptosis through activation of the cytochrome c-mediated intrinsic mitochondrial pathway. Virus Res 253:112–123

51. Kratimenos P, Koutroulis I, Agarwal B, Theocharis S, Delivoria-Papadopoulos M (2017) Effect of Src kinase inhibition on cytochrome c, Smac/DIABLO and apoptosis inducing factor (AIF) following cerebral hypoxia-ischemia in newborn piglets. Sci Rep 7:16664

52. Huang L, Yu L-J, Zhang X, Fan B, Wang F-Z, Dai Y-S, Qi H, Zhou Y, Xie L-J, Xiao S (2019) Autophagy regulates glucose-mediated root meristem activity by modulating ROS production in Arabidopsis. Autophagy 15:407–422

53. Kim W-S, Lee K-S, Kim J-H, Kim C-K, Lee G, Choe J, Won M-H, Kim T-H, Jeoung D, Lee H, Kim J-Y, Ae Jeong M, Ha K-S, Kwon Y-G, Kim Y-M (2017) The caspase-8/Bid/cytochrome c axis links signals from death receptors to mitochondrial reactive oxygen species production. Free Radic Biol Med 112:567–577

54. Davalli P, Marverti G, Lauriola A, D'Arca D (2018) Targeting oxidatively induced DNA damage response in cancer: opportunities for novel cancer therapies. Oxid Med Cell Longev 2018:2389523

Publisher's Note